

Effect of the 7-Amino Substituent on the Inhibitory Potency of Mechanism-Based Isocoumarin Inhibitors for Porcine Pancreatic and Human Neutrophil Elastases: A 1.85-Å X-ray Structure of the Complex between Porcine Pancreatic Elastase and 7-[(*N*-Tosylphenylalanyl)amino]-4-chloro-3-methoxyisocoumarin

Maria A. Hernandez,[†] James C. Powers,^{*,†} Jan Glinski,[†] Jozef Oleksyszyn,[†] J. Vijayalakshmi,[‡] and Edgar F. Meyer, Jr.[‡]

School of Chemistry and Biochemistry, Georgia Institute of Technology, Atlanta, Georgia 30332-0400, and Department of Biochemistry and Biophysics, Texas A & M University, College Station, Texas 77843-2128. Received June 17, 1991

A series of new acyl, urea, and carbonate derivatives of 7-amino-4-chloro-3-methoxyisocoumarin were synthesized and evaluated as irreversible inhibitors of human neutrophil elastase (HNE) and porcine pancreatic elastase (PPE). Inhibition of HNE is directly related to the hydrophobicity of the substituent on the 7-amino group. The *N*-Tos-Phe derivative (19) is the best HNE inhibitor with a second-order rate constant $k_{\text{obs}}/[I] = 200\,000\text{ M}^{-1}\text{ s}^{-1}$. The closest analogue in this series, the 3,3-diphenylpropionyl derivative 5, had a $k_{\text{obs}}/[I] = 130\,000\text{ M}^{-1}\text{ s}^{-1}$ with HNE. In contrast to the Tos-Phe derivative 19, phenylacetyl derivative 2 and carbonates 22 and 25 gave extremely stable enzyme-inhibitor complexes with deacylation half-lives longer than 48 h with both elastases. *N*-Phenylurea derivative 25 was the best inhibitor for PPE with a second-order rate constant $k_{\text{obs}}/[I] = 7300\text{ M}^{-1}\text{ s}^{-1}$. The crystal structure of a complex of PPE with *N*-tosyl-Phe derivative 19 was determined at 1.85-Å resolution and refined to a final *R* factor of 16.9%. The isocoumarin forms an acyl enzyme with Ser-195, while His-57 is near the inhibitor, but not covalently linked. The Tos-Phe makes a few hydrophobic contacts with the S' subsites of PPE, but appears to be interacting primarily with itself in the PPE structure. This region of HNE is more hydrophobic and modeling indicates that the inhibitor would probably make additional contacts with the enzyme.

Introduction¹

Human leukocyte (neutrophil) elastase (HNE) is a serine protease involved in inflammation and tissue degradation such as that observed in emphysema.^{2,3} Therefore, the design and synthesis of HNE inhibitors is important in the development of novel drugs having potential use in treatment of this disease. Synthetic inhibitors of serine proteases is an area of intense research and previously reported structures include ynenol lactones,⁴ oxazine-2,6-diones,⁵ benzoxazin-4-one,⁶ sulfonate salts of amino acids,⁷ trifluoromethyl ketone derivatives of amino acids and peptides,⁸ and derivatives of cephalosporins.⁹

We have recently shown that some derivatives of 3-alkoxy-4-chloroisocoumarins and 3-alkoxy-7-amino-4-chloroisocoumarins are effective and specific serine protease inhibitors.¹⁰ Both the 7-amino and 4-chloro substituents in the isocoumarin molecule are required for irreversible inhibition of the elastases by 3-alkoxy-7-amino-4-chloroisocoumarins. This is consistent with a mechanism where the isocoumarin moiety acylates serine-195 in the active site to give an acyl enzyme which can form a reactive quinonimine methide tethered to the enzyme (Scheme I). An additional covalent bond can then be formed upon alkylation of the active site His-57 by the acyl quinonimine methide to form a nondeacylateable adduct. Alternately, the quinonimine methide can react with a solvent nucleophile to give an acyl enzyme which can be deacylated by hydroxylamine treatment. Examples of both acyl enzymes and the His-57 alkylation product have been observed crystallographically in different isocoumarin complexes with PPE¹¹⁻¹³ and bovine trypsin.¹⁴ It is clear that the structural and electronic properties of different substituents on the isocoumarin ring should influence the rate of acylation of the active site serine, the reactivity of the 4-quinonimine methide which is formed, and the stability of the enzyme-inhibitor complex.

The most effective isocoumarin HNE inhibitor previously reported is 7-[(*N*-tosylphenylalanyl)amino]-4-

Scheme I

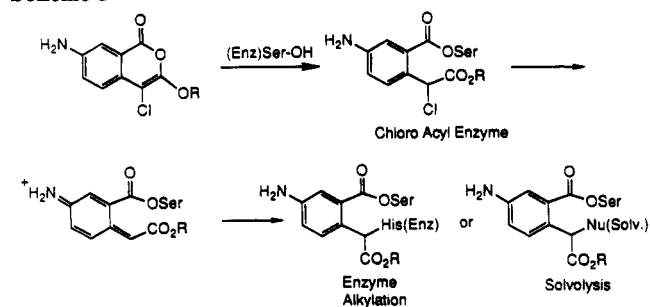
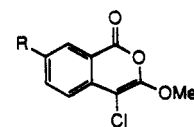


Chart I



AIC, R = H₂N

- | | |
|--|--|
| 1 R = CH ₃ CONH | 14 R = m-CH ₃ OCONHC ₆ H ₄ CONH |
| 2 R = PhCH ₂ CONH | 15 R = Tos-Ala-NH |
| 3 R = Ph ₂ CHCONH | 16 R = Tos-Val-NH |
| 4 R = PhCH ₂ CH ₂ CONH | 17 R = Tos-Leu-NH |
| 5 R = Ph ₂ CHCH ₂ CONH | 18 R = Tos-Phe-NH |
| 6 R = C ₃ F ₇ CONH | 19 R = Tos-Phe-NH |
| 7 R = HOOCCH ₂ CH ₂ CONH | 20 R = NCO |
| 8 R = HOOCCH ₂ CH ₂ CH ₂ CONH | 21 R = EtOCONH |
| 9 R = HOOCCH ₂ CHPhCH ₂ CONH | 22 R = PhOCONH |
| 10 R = o-HOOC-C ₆ H ₄ CONH | 23 R = PhCH ₂ OCONH |
| 11 R = CH ₃ OOCCH ₂ CH ₂ CONH | 24 R = Fmoc-NH |
| 12 R = CH ₃ OOCCH ₂ CH ₂ CH ₂ CONH | 25 R = PhNHCONH |
| 13 R = o-CH ₃ OOC-C ₆ H ₄ CONH | 26 R = PhCH ₂ (PhCH ₂ CH ₂)NCONH |

* To whom correspondence should be addressed.

[†] Georgia Institute of Technology.

[‡] Texas A & M University.

chloro-3-methoxyisocoumarin (19).¹⁰ The large increase in the second-order inactivation rate constant obtained by

Table I. Rate Constants ($k_{\text{obs}}/[\text{I}]$) for Inactivation of Elastases by 7-(Acylamino)-4-chloro-3-methoxyisocoumarins^a

compd no.	HLE		PPE	
	[I], μM	$k_{\text{obs}}/[\text{I}]$, $\text{M}^{-1} \text{s}^{-1}$	[I], μM	$k_{\text{obs}}/[\text{I}]$, $\text{M}^{-1} \text{s}^{-1}$
1	2.3	30 000	8.3	2 300
2	1.9	37 000	11.3	2 000
3	1.9	52 000	670.0	20
4	1.6	66 000	8.8	3 100
5	1.6	130 000	8.1	2 400
6	2.7	47 000	17.0	1 100
7	4.5	9 500	17.0	900
8	2.3	51 000	42.0	900
9	1.6	66 000	8.3	100
10	1.8	52 000	17.0	2 700
11	2.3	43 000	17.0	2 200
12	2.3	54 000	8.3	2 800
13			8.3	7 100
14	1.4	100 000	17.0	2 500

^a Conditions were as follows: 0.1 M Hepes, 0.5 M NaCl, pH 7.5 at 25 °C. Rate constants were obtained as described under Materials and Methods.

acylation of the 7-amino group in 7-amino-4-chloro-3-methoxyisocoumarin ($k_{\text{obs}}/[\text{I}] = 200\,000 \text{ M}^{-1} \text{ s}^{-1}$ for 19

- (1) Abbreviations used: HNE, Human Neutrophil Elastase; PPE, Porcine Pancreatic Elastase; TNT, Ten Eyck-Tronrud refinement package; RMS, root mean square; Phg, phenylglycine; AIC, 7-amino-4-chloro-3-methoxyisocoumarin; DMAP, 4-(*N,N*-dimethylamino)pyridine.
- (2) Bode, W.; Meyer, E., Jr.; Powers, J. C. Human Leukocyte and Porcine Pancreatic Elastase: X-Ray Crystal Structures, Mechanism, Substrate Specificity, and Mechanism-Based Inhibitors. *Biochemistry* 1989, 28, 1951–1963.
- (3) Stein, R. L.; Trainor, D. A.; Wildorger, R. A. Neutrophil Elastase. *Annu. Rep. Med. Chem.* 1985, 20, 237–246.
- (4) Tam, T. F.; Spencer, R. W.; Copp, L. J.; Krantz, A. Novel Suicide Inhibitors of Serine Proteinases. Inactivation of Human Leukocyte Elastase by Ynenol Lactones. *J. Am. Chem. Soc.* 1984, 106, 6849–6851.
- (5) Moorman, A. R.; Abeles, R. H. New Class of Serine Protease Inactivators Based on Isoic Anhydride. *J. Am. Chem. Soc.* 1982, 104, 6785–6786.
- (6) Teshima, T.; Griffin, J. C.; Powers, J. C. A New Class of Heterocyclic Serine Protease Inhibitors. Inhibition of Human Leukocyte Elastase, Porcine Pancreatic Elastase, Cathepsin G, and Bovine Chymotrypsin A₂ with Substituted Benzoxazinones, Quinazolines, and Anthranilates. *J. Biol. Chem.* 1982, 257, 5085–5091. Hedstrom, L.; Moorman, A. R.; Dobbs, J.; Abeles, R. H. Suicide Inactivation of Chymotrypsin by Benzoxazinones. *Biochemistry* 1984, 23, 1753–1759. Krantz, A.; Spencer, W. R.; Tam, F. T.; Thomas, E.; Copp, L. J. Design of Alternate Substrate Inhibitors of Serine Proteinases. Synergistic Use of Alkyl Substitution to Impede Enzyme-Catalyzed Deacylation. *J. Med. Chem.* 1987, 30, 589–591.
- (7) Groutas, W. C.; Brubaker, M. J.; Zandler, M. E.; Maso-Gray, V.; Rude, S. A.; Crowley, J. P.; Dunshee, D. A.; Giri, P. K. Inactivation of Leukocyte Elastase by Aryl Azolides and Sulfonate Salts. Structure-Activity Relationship Studies. *J. Med. Chem.* 1986, 29, 1302–1305.
- (8) Stein, R. L.; Strimpler, A. M.; Edwards, P. E.; Lewis, J. J.; Mauger, R. C.; Schwartz, J. A.; Stein, M. M.; Trainor, D. A.; Wildorger, R. A.; Zottola, M. A. Mechanism of Slow-binding Inhibition of Human Leukocyte Elastase by Trifluoromethyl Ketones. *Biochemistry* 1987, 26, 2682–2689.
- (9) Doherty, J. B.; Ashe, B. M.; Argenbright, L. W.; Barker, P. L.; Bonney, R. J.; Chandler, G. O.; Dahlgren, M. E.; Dorn, C. P.; Finke, P. E.; Firestone, R. A.; Fletcher, D.; Hagmann, W. K.; Mumford, R.; O'Grady, L.; Maycock, A. L.; Pisano, J. M.; Shah, S. K.; Thompson, K. R.; Zimmerman, M. Cephalosporin Antibiotics Can Be Modified To Inhibit Human Leukocyte Elastase. *Nature* 1986, 322, 192–194.
- (10) Harper, J. W.; Powers, J. C. Reaction of Serine Proteinases with Substituted 3-Alkoxy-4-chloroisocoumarins and 3-Alkoxy-7-amino-4-chloroisocoumarins: New Reactive Mechanism-Based Inhibitors. *Biochemistry* 1985, 24, 7200–7213.

Table II. Rate Constants ($k_{\text{obs}}/[\text{I}]$) for Inactivation of Elastases by (*N*-Tosylamino)acyl Derivatives of 7-Amino-4-chloro-3-methoxyisocoumarin^a

compd no.	HLE		PPE	
	[I], μM	$k_{\text{obs}}/[\text{I}]$, $\text{M}^{-1} \text{s}^{-1}$	[I], μM	$k_{\text{obs}}/[\text{I}]$, $\text{M}^{-1} \text{s}^{-1}$
15	1.6	55 000	8.5	2 500
16	1.6	36 000	8.4	1 300
17	1.6	54 000	8.8	6 300
18	1.6	84 000	8.3	1 500
19	1.6	200 000	8.5	6 500

^a Conditions were as follows: 0.1 M Hepes, 0.5 M NaCl, pH 7.5 at 25 °C. Rate constants were obtained as described under Materials and Methods.

compared to $10\,000 \text{ M}^{-1} \text{ s}^{-1}$ for the parent AIC) strongly indicated the importance of the substituent at this position. This finding prompted us to carry out a systematic exploration of compounds with different substituents on the 7-amino group of 7-amino-4-chloro-3-methoxyisocoumarin (AIC). In this paper we report the inactivation of HNE and PPE by a number of acyl, urea, and carbonate derivatives of AIC (Chart I). We also report a crystallographic study on the binding mode of *N*-Tos-Phe-AIC (19) complexed with PPE, which should be useful in the design of better inhibitors for both PPE and HNE.

Results and Discussion

Inactivation of Elastases by Acyl Derivatives of AIC. Fourteen *N*-acyl derivatives of AIC were prepared and tested as inactivators of HNE and PPE. The second-order inactivation rate constants ($k_{\text{obs}}/[\text{I}]$) are reported in Table I. In most cases first-order inactivation plots were linear for about two half-lives. Inactivation by these derivatives was very fast and typically only 40–60% residual enzyme activity was observed at the first time point examined (0.15–0.3 min) under the conditions given in Table I. Thus, the inactivation rate constants calculated from this residual activity should be considered to be lower limits.

In general, most of the *N*-acyl AIC derivatives were 3–7 times more reactive toward HNE than unsubstituted AIC ($k_{\text{obs}}/[\text{I}] = 10\,000 \text{ M}^{-1} \text{ s}^{-1}$). Even the product of a simple acetylation, compound 1, was a 3-fold better inhibitor. Compounds 5 and 14, which contain hydrophobic phenyl rings, were particularly strong inhibitors of HNE with $k_{\text{obs}}/[\text{I}] = 130\,000$ and $100\,000 \text{ M}^{-1} \text{ s}^{-1}$, respectively. The least reactive compound toward HNE in this series was *N*-succinyl derivative 7, which had an inactivation rate

- (11) Meyer, E. F., Jr.; Presta, L. G.; Radhakrishnan, R. Stereospecific Reaction of 3-Methoxy-4-chloro-7-amino isocoumarin with Crystalline Porcine Pancreatic Elastase. *J. Am. Chem. Soc.* 1985, 107, 4091–4093.
- (12) Powers, J. C.; Oleksyszyn, J.; Narasimhan, L. S.; Kam, C. M.; Radhakrishnan, R.; Meyer, E. F., Jr. Reaction of Porcine Pancreatic Elastase with 7-Substituted 3-Alkoxy-4-chloroisocoumarins: Design of Potent Inhibitors Using the Crystal Structure of the Complex Formed with 4-Chloro-3-ethoxy-7-guanidinoisocoumarin. *Biochemistry* 1990, 29, 3108–3118.
- (13) Vijayalakshmi, J.; Meyer, E. F., Jr.; Kam, C. M.; Powers, J. C. Structural Study of Porcine Pancreatic Elastase Complexed with 7-Amino-3-(2-bromoethoxy)-4-chloroisocoumarin as a Nonreactivable Doubly Covalent Enzyme-Inhibitor Complex. *Biochemistry* 1991, 30, 2175–2183.
- (14) Chow, M. M.; Meyer, E. F.; Bode, W.; Kam, C.-M.; Radhakrishnan, R.; Vijayalakshmi, J.; Powers, J. C. The 2.2 Å Resolution X-ray Crystal Structure of the Complex of Trypsin Inhibited by 4-Chloro-3-ethoxy-7-guanidinoisocoumarin: A Proposed Model of the Thrombin-Inhibitor Complex. *J. Am. Chem. Soc.* 1990, 112, 7783–7789.

Table III. Rate Constants ($k_{\text{obs}}/[I]$) for Inactivation of Elastases by Ureido and Urethane Derivatives of 7-Amino-4-chloro-3-methoxyisocoumarin^a

compd no.	HLE		PPE	
	[I], μM	$k_{\text{obs}}/[I]$, $\text{M}^{-1} \text{s}^{-1}$	[I], μM	$k_{\text{obs}}/[I]$, $\text{M}^{-1} \text{s}^{-1}$
20	1.8	9 200	8.3	650
21	2.3	47 000	8.3	2 000
22	1.8	13 000	8.8	850
23	1.6	71 000	140	260
24	2.5	10 000	600	20
25	2.0	49 000	8.3	7 300
26	2.2	12 000	490	17

^a Conditions were as follows: 0.1 M HEPES, 0.5 M NaCl, pH 7.5 at 25 °C. Rate constants were obtained as described under Materials and Methods.

similar to that of unsubstituted AIC. It is clear that the hydrophilic carboxyl group in 7 does not improve the interaction of the inhibitor with the enzyme. The inactivation rates with the *N*-glutaryl derivative 8, as well for methyl esters 11 and 12, were 5 times greater.

With PPE, the majority of the inhibitors were 2–3 times more reactive than nonacylated AIC. The highest $k_{\text{obs}}/[I]$ value of $7100 \text{ M}^{-1} \text{ s}^{-1}$ was obtained with the *N*-*o*-phthalyl methyl ester derivative 13. On the other hand, the lowest $k_{\text{obs}}/[I]$ value of $20 \text{ M}^{-1} \text{ s}^{-1}$ was obtained for the *N*-(di-phenylacetyl) derivative 3. Inactivation rates for the negatively charged carboxypropionamido (7), carboxybutyramido (8), and carboxybenzamido (10) compounds toward PPE were roughly 2–3 times lower than those of their methyl esters, 11, 12, and 13. Both 7 and 8 have $k_{\text{obs}}/[I]$ values close to the $1000 \text{ M}^{-1} \text{ s}^{-1}$ found for 7-amino-4-chloro-3-methoxyisocoumarin.¹⁰ This is in contrast to the large increase observed in their reactivity toward HNE.

Inactivation of Elastases by *N*-Tosyl Aminoacyl Derivatives of AIC. Four new *N*-tosyl aminoacyl derivatives of 7-amino-4-chloro-3-methoxyisocoumarin were synthesized and tested as inactivators of elastases. The second-order inactivation rate constants $k_{\text{obs}}/[I]$ are reported in Table II along with that of the previously reported phenylalanine derivative 19. First-order inactivation plots were linear for 1.5–3 half-lives. The inactivation by these derivatives was very fast. The residual enzyme activity at the first time point examined (0.12–0.15 min) ranged from 14% for 19 to 62% for 16. Therefore, the inactivation rate constants calculated from this residual activity should also be considered to be lower limits.

All of the derivatives described in Table II were much better inactivators of HNE than of PPE. The most reactive inhibitors toward HNE contained a phenyl ring (18, 19). A difference of one phenyl group was responsible for a 4-fold increase in the inactivation rate (15 and 19). On the other hand, the number of carbon atoms and/or the degree of branching in the amino acid residue did not affect the inactivation rate significantly (15–17).

The *N*-Tos-Phe derivative 19 was also one of best inhibitors for PPE; however, the presence of the phenyl group on the amino acid residue was not crucial since *N*-Tos-Leu derivative 17 was just as active. The presence of one methylene before any branching in the amino acid residue caused a 4–5-fold increase in the inactivation rate (19/18, 17/16). A carbon chain at the amino acid residue longer than one caused a 2.5-fold increase in the inactivation rate (17/15).

Inactivation of Elastases by Ureido and Urethane Derivatives of AIC. Four urethane and two urea derivatives of AIC were synthesized. The second-order inactivation rate constants ($k_{\text{obs}}/[I]$) are reported in Table III.

Table IV. Half-Lives for Deacylation of Elastases Inactivated by Isocoumarin Derivatives^a

compd no.	$t_{1/2}$, h		compd no.	$t_{1/2}$, h	
	HLE	PPE		HLE	PPE
2	>48	>48	12	1.0	1.0
7	1.5	1.3	19 ^b	10.0	
8	1.7	1.5	22	>48	>48
10	5.0	17	25	>48	>48

^a Enzyme activity was followed after removal of excess inhibitors as described in the Experimental Section. ^b Reactivation was followed without removal of excess inhibitor. Ratio of inhibitor to enzyme, $[I]/[E] = 5$. The half-life for spontaneous hydrolysis of the inhibitor was 0.34 h.

In most cases, first-order inactivation plots were linear for greater than 4 half-lives. Inactivation of elastases, especially HNE by the urethane and urea derivatives of AIC, was very rapid and typically less than 30% residual activity was observed at the first time point examined (0.15–0.3 min). Total inactivation was generally observed except in the cases of inactivation of HNE by 23 where a maximum of 60–70% inactivation was observed. In fact, this compound was the best HNE inhibitor in this series with $k_{\text{obs}}/[I] = 71000 \text{ M}^{-1} \text{ s}^{-1}$.

The inhibition rate constant for phenylurethane 22 is $13000 \text{ M}^{-1} \text{ s}^{-1}$ compared to $49000 \text{ M}^{-1} \text{ s}^{-1}$ for the corresponding phenylurea 25. This difference suggests a favorable interaction with the enzyme through hydrogen bonding of the NH in 25. A large difference is also observed in the $k_{\text{obs}}/[I]$ values of these compounds with PPE. Derivatives with very large bulky aromatic substituents (24) inactivated HNE relatively poorly and the urea 26 which contains two aromatic rings attached to the 7-amino group is also a poor inhibitor in this series. The same effect is much more evident for PPE, where 26 and 24 were the poorest inhibitors. The best PPE inhibitors again were 25 and 21, which emphasizes the similarities between these two elastases. Table III includes also 4-chloro-7-isocyanato-3-methoxyisocoumarin (20), which contains two electrophilic centers and for which it was not possible to interpret the kinetic data unequivocally in terms of the site of reaction.

Deacylation Kinetics. The half-lives for deacylation of the enzyme–inhibitor complexes after removal of excess inhibitors are summarized in Table IV. In the case of derivative 19, the recovery of enzyme activity was followed in the presence of excess inactivator. The half-life for spontaneous hydrolysis of this compound is shorter than the half-life for reactivation. Therefore these results can be compared with deacylation rates obtained with the other compounds.

In most cases, less than about 5% of the specific activity was regained during the centrifugation period and this is consistent with formation of a covalent enzyme–inhibitor adduct. Further standing of some of the enzyme–inhibitor adducts at 25 °C resulted in slow deacylation of the acyl enzymes with recovery of enzyme activity. Deacylation of elastases was relatively faster when the inactivators were alkylacyl derivatives (7, 8, and 12) than when the inactivators had aromatic groups; no deacylation was observed with enzymes inactivated by 2, 22, and 25 after standing for at least 48 h. These slow deacylation rates are consistent with the formation of His alkylation products (Scheme 1). The best inhibitor, compound 19, had a moderate deacylation half-life of 10 h.

X-ray Crystallographic Study of the Binding Mode of *N*-Tos-Phe-AIC (19) with PPE. A crystallographic study of Tos-Phe-AIC (19) bound to PPE unambiguously shows covalent binding of the inhibitor to the enzyme

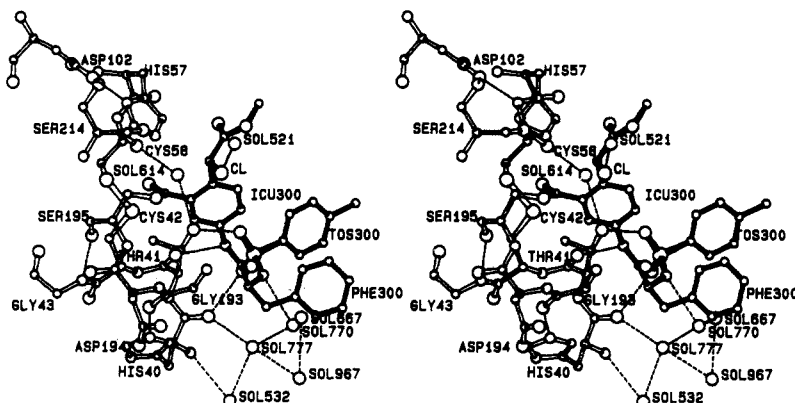


Figure 1. Program ballstick (R. Radhakrishnan, unpublished) was used to create the stereo view of the title complex including relevant H bonds.

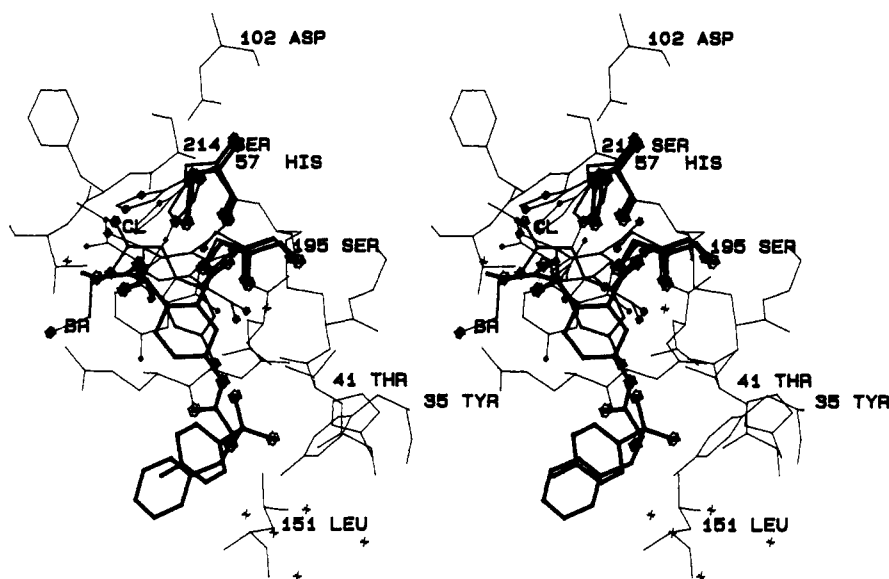


Figure 2. Stereo superposition and comparison of the binding modes of four PPE-isocoumarin complexes. The active site residues in the title complex are drawn in stereo. The figure was obtained using FRODO with the BLOB radius for the title inhibitor set at 0.3 Å (heavy lines), for 7-amino-3-(2-bromoethoxy)-4-chloroisocoumarin structure at 0.3 Å (thin lines), for 4-chloro-3-ethoxy-7-guanidinoisocoumarin at 0.20 Å (medium lines, Cl labeled in the S_1 pocket) and for 7-amino-4-chloro-3-methoxyisocoumarin structure at 0.1 Å (thin lines). The complexity resulting from the superposition of all PPE-isocoumarin complexes is unavoidable; the viewer may be assisted by viewing the complexes in stereo and by searching for the characteristic phenyl ring of each complex; the "downward" displacement of the Tos-Phe complex is clearly seen, relative to the "upper" displacement of the doubly bound (to Ser-195 and His-57) complex of the bromoethoxyisocoumarin with PPE. Comparison of active site backbone atoms shows that virtually no displacement of active site backbone atoms occurs, rather, the His-57 and Ser-195 side chain atoms undergo torsional shifts to provide the required flexibility.

corresponding to the chloro acyl enzyme structure shown in Scheme I. The electron density map has continuous density corresponding to the ester covalent linkage formed between Ser-195 O_γ and the benzoyl carbonyl carbon atom of the inhibitor. In addition to the covalent linkage between the enzyme and the inhibitor, the complex is further stabilized by hydrogen bonding. The final refined model of the active site, including hydrogen bonding, is given in Figure 1.

The important hydrogen-bonding interactions observed in the Tos-Phe-AIC complex are given in Table V. The amino nitrogen atom at the 7-position of the isocoumarin ring forms a hydrogen bond (2.75 Å) with the carbonyl oxygen of Thr-41, similar to the one observed in the 7-amino-3-(2-bromoethoxy)-4-chloroisocoumarin complex with PPE.¹³ The guanidino group in the complex of PPE with 4-chloro-3-ethoxy-7-guanidinoisocoumarin also forms hydrogen bonds with Thr-41.¹² The oxygen atoms of the tosyl group forms two hydrogen bonds to the enzyme (one from O_6 of the tosyl group to the carbonyl oxygen atom

of His-40 (2.84 Å) and the other from O_5 of the tosyl group to the O_γ of Thr-41 (2.61 Å), which adds to the stability of the tosyl group in the PPE active site. There is also an interesting hydrogen-bonding network involving five solvent molecules, the carbonyl oxygen atom of His-40, the amido nitrogen atom of the phenylalanyl group, and the O_6 atom of the tosyl group.

The isocoumarin phenyl ring is markedly displaced from the active site, relative to other isocoumarin complexes (Figure 2). This allows the imidazole ring of His-57 imidazole ring to remain in the "in" position, retaining its "standard" H-bonding interactions with the catalytic tetrad as well as providing a snug fit for nearby portions of the inhibitor (Figure 1). The distance of Ser-195 O_γ from His-57 $N\epsilon_2$ is 3.3 vs 3.2 Å found between these two atoms in the native structure.¹⁵

(15) Meyer, E. F., Jr.; Cole, G.; Radhakrishnan, R.; Epp, O. Structure of Native Porcine Pancreatic Elastase at 1.65 Å Resolution. *Acta Crystallogr.* 1988, *B44*, 26-38.

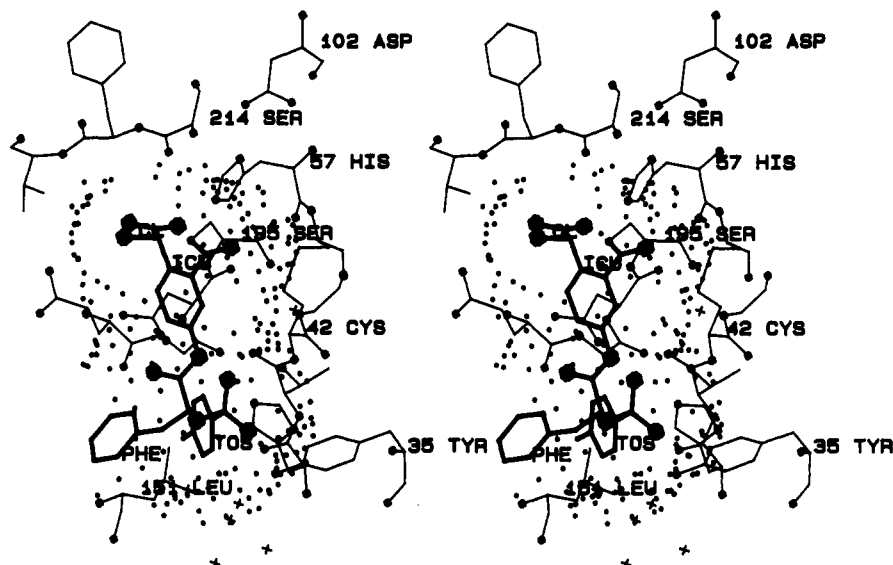


Figure 3. The contact surface (defined as the locus of points within 2 Å of all protein atoms in contact with the double van der Waals radius of all inhibitor atoms) is drawn in stereo with the INTER option of program FRODO. Favorable interactions are exhibited by those receptor atoms situated on the interaction surface (e.g. Cys-42-Cys-58 disulfide atoms, His-57 N ϵ 2, Tyr-35 OH). For drug-design purposes, such figures reveal regions for synthetic enhancement of binding; e.g. the methoxy group at the top could be extended for additional contacts with the extended substrate binding site (e.g. the peptide chain of residues 214–216 which forms an antiparallel β -sheet structure with the substrate). This figure clearly shows that solvent (HOH) is excluded from the oxyanion hole by the van der Waals bulk of the inhibitor.

Table V. Hydrogen Bonds (Å) in the Active Site of the Complex of Tos-Phe-AIC with PPE

Icu N1 ^a	Thr 41 carbonyl O	2.75
Tos O6	His 40 carbonyl O	2.84
Tos O5	Thr 41 O γ 1	2.61
Phe N2	Sol 770 OH	3.12
SOL 770 OH	Sol 777 OH	2.68
SOL 777 OH	His 40 carbonyl O	2.78
SOL 770 OH	SOL 667 OH	3.10
SOL 667 OH	SOL 967 OH	3.10
SOL 777 OH	SOL 967 OH	2.99
SOL 777 OH	SOL 532 OH	3.06
HIS 40 NH	Sol 532 OH	3.13
SOL 614 OH	Thr 41 O γ 1	2.86
SOL 614 OH	Cys 58 carbonyl O	2.69
Gly 43 NH	Ser 195 carbonyl O	2.77
Icu Cl	Sol 521 OH	2.95
Ser 195 O γ	His 57 N ϵ 2	3.30
His 57 N δ 1	Asp 102 O δ 1	2.60
Asp 102 O δ 1	Ser 214 O γ	2.80

^a Icu = 7-aminoisocoumarin ring atoms.

The imidazole ring of His-57 has been forced into the "out" conformation in all previously determined PPE-isocoumarin complexes by van der Waals contacts with the inhibitor.^{11–13} In the complex of PPE with 7-amino-3-(2-bromoethoxy)-4-chloroisocoumarin,¹³ the "in" conformation corresponded to formation of a covalent linkage (His-57 N ϵ 2-isocoumarin C4) with the inhibitor (enzyme alkylation in Scheme I). Surprisingly, in the present structure the His-57 imidazole ring is still found in the "in" position even though there is only a single covalent link between the isocoumarin and O γ of Ser-195. One difference between this structure and the earlier (bromoethoxy)isocoumarin complex with PPE is a tilt of the His-57 imidazole ring in the bromoethoxy structure approximately 30° away from Asp-102 with respect to the ring orientation in the native structure. This tilt is due to inhibitor binding and causes an unfavorable angle for hydrogen bonding between Asp-102 O δ 1 and His-57 N δ 1 (donor–H–acceptor angle = 110°) although the distance between them is 3.05 Å. In the Tos-Phe complex, the His-57 imidazole ring is almost parallel to the geometry in the native structure and thus

the hydrogen bonding (2.82 Å; donor–H–acceptor = 152°) between His-57 N δ 1 and Asp-102 O δ 1 is similar to that found in the native structure. It is possible that the tilt of the histidine ring along with the low pH of the crystallographic experiments is responsible for the absence of a histidine alkylation product in the Tos-Phe crystal structure.

The chlorine atom in the chloro acyl enzyme structure is inserted into the S₁ pocket (subsite nomenclature of Schechter and Berger)¹⁶ formed by portions of residues Cys-191, Gln-192, Gly-193, Ser-195, Thr-213, Ser-214, Phe-215, Val-216, Thr-226, and Val-227. The isocoumarin has not reacted with His-57, although the His-57 is only 3.1 Å removed from the carbon of the C–Cl bond. The highly electronegative Cl atom makes a hydrogen bond (2.95 Å) with a nearby solvent molecule in the active site. It is interesting to note that the chlorine atom in the complex of a 5-chlorobenzoxazinone derivative with PPE was also found to occupy the S₁ pocket.¹⁷ Other van der Waals contacts between PPE and the inhibitor are shown in Figure 3.

In the four isocoumarin complexes of PPE that have been studied so far crystallographically, only the 7-amino-4-chloro-3-methoxyisocoumarin complex of PPE has its benzoyl carbonyl oxygen atom partially in the oxyanion hole located between the amide (>NH) groups of Gly-193 and Ser-195. In the other three PPE structures, namely 4-chloro-3-ethoxy-7-guanidinoisocoumarin,¹² 7-amino-3-(2-bromoethoxy)-4-chloroisocoumarin,¹³ and the present structure, the benzoyl carbonyl oxygen atom is displaced from the oxyanion hole. The benzoyl carbonyl oxygen atom in the present structure is pointing approximately in the same direction as that in the 4-chloro-3-ethoxy-7-

(16) Schechter, I.; Berger, A. On the Size of the Active Site in Proteases. *Biochem. Biophys. Res. Commun.* 1967, 27, 157–162.

(17) Radhakrishnan, R.; Presta, L. G.; Meyer, E. F., Jr.; Wildonger, R. Crystal Structures of the Complex of Porcine Pancreatic Elastase with Two Valine-derived Benzoxazinone Inhibitors. *J. Mol. Biol.* 1987, 198, 417–424.

guanidinoisocoumarin-PPE complex, suggesting that this is a preferred conformation and may explain the slow deacylation rates of the acyl isocoumarins.

The methoxy group of the ester formed from the isocoumarin ring is oriented in the same way in the Tos-Phe structure (Figures 2 and 3) as the bromoethoxy group in the recently solved doubly covalently bound complex of 7-amino-3-(2-bromoethoxy)-4-chloroisocoumarin with PPE.¹³ The CH₃OCO group is located near the entrance to the S₁ pocket, but is directed away from the enzyme into solution and does not make any significant interactions with the enzyme. The Tos-Phe group at the 7-position points toward the S₂' subsite comprised of portions of residues His-40, Thr-41, Leu-143, Leu-151, Gln-192, and Gly-193. The phenylalanyl residue connected to the 7-amino nitrogen of the isocoumarin is located in the S₂' subsite. There are a few van der Waals interactions of the phenyl group of phenylalanyl residue with Leu-151, primarily involving the methylene group of the benzyl side chain. The tosyl group is situated very close to the S₁' subsite formed from portions of Thr-41, Cys-42-S-S-Cys-58, Arg-61, Leu-63, Phe-65, but the tosyl ring occupies regions common to both the S₁' and the S₂' subsites. The hydroxyl group of Tyr-35 is pointed toward the tosyl ring and makes van der Waals interactions with the tosyl aromatic carbons located in the range of 3.3–3.6 Å from the Tyr-35 oxygen. Most of the hydrophobic interactions of the Tos-Phe group appear to be between the Tos aromatic group and the Phe aromatic ring with carbon-carbon distances ranging from 3.2 to 3.7 Å. The Leu-151, the phenyl group of the Phe, the tosyl group, and Tyr-35 form a hydrophobic sandwich with the Phe phenyl shielding the Tos group from solvent.

Conclusion

The crystal structure of the Tos-Phe-AIC complex with PPE has allowed interpretation of many of the kinetic results which have been obtained with PPE. Phenylurea **25** ($k_{\text{obsd}}/[\text{I}] = 7300 \text{ M}^{-1} \text{ s}^{-1}$) is the best PPE isocoumarin inhibitor for PPE found in the present study and is among the best ones known in the literature.¹⁸ The phenyl group of **25** can interact with Leu-151 and the PhNH can form an additional hydrogen bond with the carbonyl group of Thr-41 and/or His-40. The corresponding urethane **22** which cannot form these hydrogen bonds is a much poorer inhibitor ($k_{\text{obsd}}/[\text{I}] = 850 \text{ M}^{-1} \text{ s}^{-1}$). The *o*-phthalyl methyl ester derivative **13** is also an effective PPE inhibitor ($k_{\text{obsd}}/[\text{I}] = 7100 \text{ M}^{-1} \text{ s}^{-1}$) since the phenyl group can also interact with Leu-151, while the MeOCO oxygens can form the same hydrogen bonds as the sulfonyl oxygens in the Tos group of the Tos-Phe structure. The *N*-Tos-Leu derivative **17** ($k_{\text{obsd}}/[\text{I}] = 6300 \text{ M}^{-1} \text{ s}^{-1}$) is nearly as effective as the *N*-Tos-Phe-AIC derivative **19** ($k_{\text{obsd}}/[\text{I}] = 6500 \text{ M}^{-1} \text{ s}^{-1}$) and can make the same interactions observed in the crystal structure. The hydrophobic sandwich of Leu-151, the phenyl group of the Phe residue, the tosyl group, and Tyr-35 would not be as favorable with the Tos-Ala (too small), Tos-Val (too small), or Tos-Phe (too crowded) derivatives. Interestingly the PhCH₂(PhCH₂CH₂)NCO-AIC derivative (**26**), which is similar to the Tos-Phe derivative **19** in overall shape (e.g. **19** = PhCH₂-(MePhSO₂NH)CHCO-AIC), is a very poor inhibitor ($k_{\text{obsd}}/[\text{I}] = 17 \text{ M}^{-1} \text{ s}^{-1}$). We propose that the nitrogen from which the two arylalkyl groups branch in **26** results in a more planar inhibitor geometry in this region of the PPE active site and poorer enzyme-inhibitor interactions.

All of the isocoumarin inhibitors are much better HNE inhibitors, and those inhibitors such as **19** which have hydrophobic acyl groups attached to the isocoumarin 7-amino group are particularly potent inhibitors. The S' subsites of HNE are much more hydrophobic than those in PPE due to the following changes: Thr-41 to Phe-41 in HNE, Tyr-35 to Leu-35, and Gln-192 to Phe-192. Thus, we propose that the Tos-Phe group of the inhibitor will make a much better hydrophobic sandwich in the HNE active site. This is a result not only of the sequence changes but also is due to small movements of residues such as Leu-143, which results in slightly better contacts with the inhibitor.

Most simple serine proteases including PPE are "lock and key" enzymes¹⁹ and do not significantly change their conformation upon inhibitor binding. With PPE, the root mean square (RMS) deviation ranges from 0.16 to 0.23 Å upon comparison of the backbone atoms in the various inhibitor complexes with each other or native PPE. On the other hand human thrombin exhibits much greater flexibility and the insertion loop undergoes substantial conformational changes upon inhibitor binding.²⁰

Finally, it should be noted that a wide variety of binding modes and reaction products have been observed in complexes of isocoumarins with serine proteases. The structures of four isocoumarin complexes with PPE have now been determined crystallographically. These structures include three different reaction products and four significantly different binding geometries. Nevertheless, these structures have been invaluable in understanding the binding mode of isocoumarins to serine proteases and should be useful in the design of more potent inhibitors for elastases.

Experimental Section

Synthesis. All common chemicals and solvents were reagent grade or better. The purity of each compound was checked by ¹H NMR spectroscopy, mass spectroscopy, thin-layer chromatography (TLC), and elemental analysis, and results are consistent with the proposed structures. The ¹H NMR were recorded on either a Varian-T60 or a Bruker WM 300 MHz instrument. Mass spectra were recorded on a Varian Mat 112s spectrometer. Elemental analyses were performed by Atlantic Microlabs of Atlanta, GA. Thin-layer chromatographic analyses (TLC) were conducted on silica gel plates with CH₃OH-CHCl₃ (1:9) as eluent.

4-Nitrohomophthalic acid was obtained from homophthalic acid.²¹ Methyl 2-carboxy-4-nitrophenylacetate was obtained by esterification of the preceding acid with methanol for 3 h at 50 °C in the presence of a catalytic amount of concentrated H₂SO₄. 7-Nitro-4-chloro-3-methoxyisocoumarin was obtained similarly to the procedures given by Tirodkar and Usgaonkar²² and its reduction on 5% Pd/C in EtOAc/MeOH gave 7-amino-4-chloro-3-methoxyisocoumarin.

7-(Acetylamino)-4-chloro-3-methoxyisocoumarin (1). A solution containing 700 mg of AIC in 15 mL of dry THF was treated with 2 mL of Ac₂O and 5 mg of DMAP. In 5 min crystals of the acylated compounds started to precipitate. After 3 h, the reaction mixture was concentrated to about 5 mL and filtered. The collected crystals were washed with acetone and dried, giving

(18) Powers, J. C.; Harper, J. W. *Proteinase Inhibitors*; Barrett, A. J., Salvensen, G., Eds.; Elsevier: Amsterdam, 1986; pp 55–152.

(19) Fischer, E. Influence of Configuration on the Activity of Enzymes. *Ber. Deutsch. Chem. Ges.* 1894, 27, 2985–2993.
 (20) Bode, W.; Mayr, I.; Baumann, U.; Huber, R.; Stone, S. R.; Hofsteenge, J. The Refined 1.9 Å Crystal Structure of Human α-Thrombin: Interaction with D-Phe-Pro-Arg Chloromethyl ketone and Significance of the Tyr-Pro-Pro-Trp Insertion Segment. *EMBO J.* 1989, 8, 3467–3475.
 (21) Choksey, J.; Usgaonkar, R. N. Isocoumarins: Part XV. 7-Nitro and 7-Amino Isocoumarins from 4-Nitrohomophthalic Acid. *Indian J. Chem. Sect. B.* 1976, 14B, 596–598.
 (22) Tirodkar, R. B.; Usgaonkar, R. N. Isocoumarins. VI. 3-Alkoxy-4-chloroisocoumarins. *Indian J. Chem.* 1969, 7, 1114–1116.

680 mg (82%); mp >210 °C dec; MS *m/e* 267 (M⁺). Anal. (C₁₂H₁₀ClNO₄) C, H, N, Cl.

Amides of 7-Amino-4-chloro-3-methoxyisocoumarin (Acylation with Acid Chlorides). Amides 2–6 and 14 were obtained by the acylation of AIC with the appropriate acid chlorides. If the acid chlorides were not commercially available, they were prepared by refluxing the corresponding acid with a 4-fold excess of SOCl₂ followed by evaporation of dryness. No additional purification of the chlorides was required. In a typical experiment AIC (1 equiv) and the acid chloride (1.5 equiv) were dissolved in THF, and then Et₃N (1.5 equiv) was added dropwise to the stirred mixture over a period of 4 h. After addition of Et₃N was completed, the reaction mixture was stirred for 20 h at room temperature; then the solvent was removed in vacuo and the residue dissolved in ethyl acetate. This solution was washed with an equal volume of water, 10% aqueous citric acid, 4% aqueous NaHCO₃, and finally again with water, dried over MgSO₄, and evaporated. The residue was crystallized from THF/hexane or from acetone.

7-[(Phenylacetyl)amino]-4-chloro-3-methoxyisocoumarin (2): pale yellow solid; yield 60%; mp 206–207 °C; MS *m/e* 343 (M⁺). Anal. (C₁₈H₁₄ClNO₄) C, H, N, Cl.

7-[(Diphenylacetyl)amino]-4-chloro-3-methoxyisocoumarin (3): pale yellow crystals; yield 45%; mp 204–205 °C; MS *m/e* 419 (M⁺). Anal. (C₂₄H₁₈ClNO₄) C, H, N, Cl.

7-[(3-Phenylpropionyl)amino]-4-chloro-3-methoxyisocoumarin (4): yellow solid (recrystallized from THF/H₂O); yield 44%; mp 211–212 °C dec; MS *m/e* 357 (M⁺). Anal. (C₁₉H₁₆ClNO₄) C, H, N.

7-[(3,3-Diphenylpropionyl)amino]-4-chloro-3-methoxyisocoumarin (5): yellow plates (crystallized from acetone/water); yield 54%; mp 220–221 °C; MS *m/e* 433 (M⁺). Anal. (C₂₅H₃₀ClNO₄·H₂O) C, H, N.

7-[(Heptafluorobutyryl)amino]-4-chloro-3-methoxyisocoumarin (6): yellow solid; yield 62%; mp 189–190 °C; MS *m/e* 421 (M⁺). Anal. (C₁₄H₇F₇ClNO₄) C, H, N.

7-[[3-[N-(Methoxycarbonyl)amino]benzoyl]amino]-4-chloro-3-methoxyisocoumarin (14): orange solid; yield 85%; mp 240–242 °C dec; MS *m/e* 402 (M⁺). Anal. (C₁₉H₁₅ClN₂O₆) C, H, N, Cl.

Reaction of Isocoumarin with Cyclic Anhydrides. One gram of AIC, dissolved in 15 mL of pyridine was treated with 4 equiv of the anhydride. After 20 min, 3 mL of water was added to the reaction mixture. Partial evaporation of the solvents left a semisolid residue, which was diluted with a mixture of acetone and water (3:1) and filtered. The crude crystals were then recrystallized from acetone (about 500 mL) to give pale yellow crystals. Yields generally were above 70%.

7-(3-Carboxypropionamido)-4-chloro-3-methoxyisocoumarin (7): yellow solid; mp 225–227 °C dec; MS *m/e* 325 (M⁺). Anal. (C₁₄H₁₂ClNO₆) C, H, N, Cl.

7-(4-Carboxybutyramido)-4-chloro-3-methoxyisocoumarin (8): yellow solid; mp 194 °C dec; MS *m/e* 339 (M⁺). Anal. (C₁₅H₁₄ClNO₆) C, H, N, Cl.

7-(4-Carboxy-3-phenylbutyramido)-4-chloro-3-methoxyisocoumarin (9): In this case, the reaction time was 5 h: yellow solid (recrystallized from acetone/H₂O); yield 62%; mp 105–106 °C; MS (FAB⁺) *m/e* 416 (M⁺ + 1). Anal. (C₂₁H₁₈ClNO₆·H₂O) C, H, N.

7-(*o*-Carboxybenzamido)-4-chloro-3-methoxyisocoumarin (10): yellow solid; mp 208 °C dec; MS *m/e* 373 (M⁺). Anal. (C₁₈H₁₂ClNO₆) C, H, N, Cl.

Methyl Esters of 7, 8, and 10. An ethereal solution containing 2.5 mmol of diazomethane was added to a solution of 0.6 mmol of the acid dissolved in a mixture of DMF and ethyl acetate. After 30 min the reaction mixture was evaporated to dryness and the crude ester recrystallized from acetone giving in each case greater than 75% yield of the methyl ester.

7-[(Methoxysuccinyl)amino]-4-chloro-3-methoxyisocoumarin (11): yellow solid; mp 221–223 °C dec; MS *m/e* 339 (M⁺). Anal. (C₁₆H₁₄ClNO₆) C, H, N, Cl.

7-[(Methoxyglutaryl)amino]-4-chloro-3-methoxyisocoumarin (12): yellow solid; mp 147–151 °C dec; MS *m/e* 353 (M⁺). Anal. (C₁₆H₁₆ClNO₆) C, H, N, Cl.

7-[(*o*-Methoxyphthalyl)amino]-4-chloro-3-methoxyisocoumarin (13): yellow solid; mp 213–216 °C dec; MS *m/e* 387

(M⁺). Anal. (C₁₉H₁₄ClNO₆) C, H, N, Cl.

7-[(*N*-Tosylalanyl)amino]-4-chloro-3-methoxyisocoumarin (15). *N*-Tosylalanine acid chloride (prepared as described below, 86 mg, 0.33 mmol) and AIC (50 mg, 0.22 mmol) were reacted as described below. After recrystallization from THF/H₂O, 15 was obtained as a pale yellow solid (59.3 mg, 60%); mp 225–226 °C; MS *m/e* 450 (M⁺). Anal. (C₂₀H₁₉ClN₂O₆S) C, H, N.

7-[(*N*-Tosylvalyl)amino]-4-chloro-3-methoxyisocoumarin (16). *N*-Tosylvaline (0.5 g, 1.8 mmol) was dissolved in 2 mL of SOCl₂ and stirred at reflux temperature for 40 min. The reaction mixture was concentrated to dryness in vacuo and the residue triturated with EtOAc/hexane (3:1) to yield the acid chloride (0.5 g, 94%) which is used in the next step without further purification. *Tos*-Val-Cl (80 mg, 0.28 mmol) and AIC (50 mg, 0.22 mmol) were dissolved in a mixture of methylene chloride (1 mL) and THF (1 mL). A solution of triethylamine (0.04 mL in 2 mL of CH₂Cl₂) was added dropwise and the reaction mixture was stirred at room temperature for 2 h. The solvent was removed in vacuo and the residue was triturated with ethyl acetate (1.5 mL). The resulting yellow solid was recrystallized from THF/H₂O to yield 38.5 mg (37%) of 16: mp 267–269 °C dec; MS *m/e* 478 (M⁺). Anal. (C₂₂H₂₃ClN₂O₆S) C, H, N.

7-[(*N*-Tosylleucyl)amino]-4-chloro-3-methoxyisocoumarin (17). *N*-Tosylleucine acid chloride (prepared as above, 100 mg, 0.33 mmol) and AIC (50 mg, 0.22 mmol) were reacted as described above. After recrystallization from acetone/water, 60 mg (55%) of 17 was obtained: mp 247–248 °C dec; MS *m/e* 492 (M⁺). Anal. (C₂₃H₂₅ClN₂O₆S) C, H, N.

7-[(*N*-Tosyl- α -phenylglycyl)amino]-4-chloro-3-methoxyisocoumarin (18). A mixture of *N*-tosyl- α -phenylglycine acid chloride (155 mg) and AIC (72 mg, 0.32 mmol) was treated as described above. After recrystallization from THF/H₂O, 18 was obtained as yellow needles: 108 mg (66%); mp 150–151 °C dec; MS *m/e* 512 (M⁺). Anal. (C₂₅H₂₁ClN₂O₆S) C, H, N.

7-[(*N*-Tosylphenylalanyl)amino]-4-chloro-3-methoxyisocoumarin (19). A mixture of *N*-tosylphenylalanine acid chloride (61 mg, 0.33 mmol) and AIC (50 mg, 0.22 mmol) was treated as described above. After recrystallization from acetone/H₂O, 19 was obtained as a yellow solid (41 mg, 35%); mp 223–224 °C dec; MS *m/e* 526 (M⁺). Anal. [C₂₆H₂₃ClN₂O₆S·0.5H₂O] C, H.

7-Isocyanato-4-chloro-3-methoxyisocoumarin (20). A solution of AIC (500 mg, 2.2 mmol) in 40 mL of dry THF was added dropwise over 20 min into a solution of phosgene in THF. The reaction mixture was stirred at room temperature for 40 min and then the excess phosgene was removed in vacuo through a KOH trap. Removal of the solvent in vacuo affords the product as a yellow solid which was used in subsequent steps without further purification (550 mg, 98%); mp 220–222 °C dec; MS *m/e* 251 (M⁺). Anal. [C₁₁H₉ClNO₄·1.65H₂O] C, H, N.

7-[(Ethoxycarbonyl)amino]-4-chloro-3-methoxyisocoumarin (21). A solution of 300 mg (1.33 mmol) of AIC in 30 mL of dry THF was treated with 432 mg (4.0 mmol) of ethyl chloroformate and 202 mg (2.0 mmol) of triethylamine. The reaction mixture was stirred for 3 days at room temperature and, after that time, was evaporated, and the dry residue was treated with a solution of 400 mg of K₂CO₃ in 5 mL of H₂O and extracted with 20 mL of chloroform. The chloroform extract was dried with Na₂SO₄ and concentrated to about 2 mL, giving 83 mg (21%) of 21 as red crystals: mp 154–157 °C dec; MS *m/e* 297 (M⁺). Anal. (C₁₃H₁₂ClNO₆) C, H, N, Cl.

7-[(Phenoxycarbonyl)amino]-4-chloro-3-methoxyisocoumarin (22). A mixture of 450 mg (2 mmol) of AIC and 468 mg (3 mmol) of phenoxycarbonyl chloride were suspended in 20 mL of THF/benzene 1:1 and then triethylamine (0.4 mL, 3 mmol) in 5 mL of THF was added dropwise with stirring during 4 h. The reaction mixture was stirred overnight at room temperature, and then 50 mL of benzene and 100 mL of ethyl acetate were added. The solution was washed with water, 10% citric acid, 4% NaHCO₃, and water, dried over MgSO₄, and concentrated. The residue was crystallized from THF/hexane to give 22 as a pale yellow solid (450 mg, 65%); mp 182–184 °C dec; MS *m/e* 345 (M⁺). Anal. (C₁₇H₁₂ClNO₆) C, H, N, Cl.

7-[(Benzyloxy)carbonyl]amino]-4-chloro-3-methoxyisocoumarin (23). The reaction of 450 mg (2.0 mmol) of AIC and 510 mg (3.0 mmol) of benzyl chloroformate was carried out as described above to yield 380 mg (51.4%) of 23 as a pale yellow

solid; mp 169–171 °C; MS *m/e* 359 (M^+). Anal. ($C_{18}H_{14}ClNO_5$) C, H, N, Cl.

7-[[**(9-Fluorenylmethoxy)carbonyl**amino]-4-chloro-3-methoxyisocoumarin (24). The reaction of 450 mg (2.0 mmol) of AIC and 776 mg (3.0 mmol) of 9-fluorenylmethyl chloroformate was carried out as described above to yield 360 mg (40%) of 24 as a pale yellow solid: mp 199–201 °C; MS *m/e* 447 (M^+). Anal. ($C_{25}H_{18}ClNO_5$) C, H, N, Cl.

7-[[**(*N*-Phenylcarbonyl)amino**]-4-chloro-3-methoxyisocoumarin (25). This compound was prepared by reaction of 110 mg (0.5 mmol) of AIC with 60 mg (0.5 mmol) of phenyl isocyanate at room temperature in CH_2Cl_2 for 24 h. After standard workup 25 was obtained as yellow crystals: mp 203–204 °C; MS *m/e* 344 (M^+). Anal. ($C_{17}H_{13}ClN_2O_4$) C, H, N, Cl.

7-[[**(*N*-Benzyl-*N*-phenethylcarbonyl)amino**]-4-chloro-3-methoxyisocoumarin (26). A solution of 0.26 mL (2.0 mmol) of triethylamine in 5 mL of benzene was added to a mixture of 503 mg (2.0 mmol) of 20 and 493 mg (2.0 mmol) of *N*-(2-phenylethyl)benzylamine hydrochloride in 20 mL of THF during a period of 3 h. The mixture was stirred overnight at room temperature and then standard workup gave 26 as a yellow solid (520 mg, 56%): mp 145–146 °C; MS *m/e* 462 (M^+). Anal. ($C_{26}H_{23}ClN_2O_4$) C, H, N, Cl.

Enzyme Inhibition Kinetics—Materials and Methods. HNE was a generous gift from Dr. James Travis and his research group at the University of Georgia. PPE was purchased from Sigma Chemical Co. (St. Louis, MO) and was of the highest purity available. Hepes, 4-(2-hydroxyethyl)-1-piperazineethanesulfonic acid, was purchased from Aldrich Chemical Co. (Milwaukee, WI). MeO-Suc-Ala-Ala-Pro-Val-NA²³ and Suc-Ala-Ala-Ala-NA²⁴ were prepared as previously described.

Enzyme Inactivation. Inactivation was initiated by adding a 25–50- μ L aliquot of inhibitor in Me_2SO to 0.5 mL of a buffered enzyme solution (0.1–2.0 μ M) such that final Me_2SO concentration was 8–12% v/v at 25 °C. Aliquots were removed with time and diluted into substrate solution (40–200-fold dilution), and the residual activity was measured spectrophotometrically as described below. Unless otherwise noted, 0.1 M Hepes and 0.5 NaCl (pH 7.5) buffer was utilized throughout, and inhibitor concentrations are shown in the appropriate table. All spectrophotometric measurements were carried out on either a Beckman 25, Beckman 35, or Varian DMS-90 spectrophotometer.

HNE was assayed with MeO-Suc-Ala-Ala-Pro-Val-NA (0.1–0.125 mM)²³ and PPE was assayed with Suc-Ala-Ala-Ala-NA (0.6–1.2 mM).²⁴ Peptide 4-nitroanilide hydrolysis was measured at 410 nm ($\epsilon_{410} = 8800 M^{-1} cm^{-1}$).²⁵ First-order inactivation rate constants (k_{obs}) were obtained from plots of $\ln(v_t/v_0)$ vs time.

Deacylation Kinetics. The deacylation rate of an enzyme-inhibitor complex was monitored by measuring enzymatic activity with time upon standing of the incubation solution without removal of excess inhibitors if half-times for spontaneous hydrolysis of the inhibitor were shorter than the deacylation rate. The deacylation rate of the inactivation enzymes (<10% activity) in most cases was measured after the removal of excess inhibitors by centrifugation with Centricon-10 microconcentrators twice at 0 °C for 1 h, and enzymatic activity of the solution upon standing at 25 °C was assayed as described above. The first-order deacylation rate (k_{deacyl}) was obtained from plots of $\ln(v_0 - v_t)$ vs time, where v_0 is the enzymatic rate under the same conditions without inhibitor.

Determination of Spontaneous Hydrolysis Rate of Inhibitors in Buffer Solutions. An aliquot of isocoumarin derivative (0.015–0.10 mM final concentration) in Me_2SO was added to the appropriate buffer solution such that the final concentration

of Me_2SO was 10% v/v, and the spontaneous hydrolysis was monitored by following the decrease in absorbance at 350 nm. The hydrolysis product had negligible absorbance at this wavelength. First-order hydrolysis rate constants were obtained from plots of $\ln[(A_t - A_\infty)/(A_0 - A_\infty)]$ vs time where A_t and A_∞ are absorbance after time t and at the end of the reaction. These constants were converted to half-lives.

X-ray Crystallography Study. A solution of PPE and the *N*-Tos-Phe derivative 19 was allowed to react in 0.1 M sodium phosphate buffer at pH 5.0 with 7% acetonitrile. The ratio of inhibitor to enzyme was 7:1 and the concentration of the enzyme was 1.2% (w/v). After 5 days crystals of the inhibited enzyme were obtained by vapor diffusion from 0.1 M sodium phosphate and 0.1 M sodium sulfate solution. A crystal of dimension 0.5, 0.4, 0.5 mm was chosen for data collection. The crystal was mounted in a capillary in contact with traces of buffer and a small quantity of fresh, solid inhibitor. Diffraction data were collected in 10 days using the rotation method with a flat-plate precession camera modified for oscillation photography (Huber-Rimsting Model 206). For data collection, a Rigaku RU-200 generator operating at 45 kV and 180 mA and equipped with a doubly bent, focusing graphite monochromator was used for data collection; a 0.3-mm collimator was used. Data collection was carried out at –5 °C with a crystal rotation rate of 3°/330 min over the rotation range of 74° on the spindle axis, with a crystal to film distance of 50 mm and with the crystal *C* axis approximately along the rotation axis. The misalignment in the crystal mounting was –7° and –25° with respect to the *y* and *z* camera axes.

The reflection intensities were measured using an Optronics P-1000 microdensitometer. The crystal cell dimensions and the missetting angles were refined using the program MADNES.²⁶ The intensities were evaluated using the program FILME²⁷ to evaluate screenless precession or rotation films of protein crystals. Data to 1.85-Å resolution contained 13 872 unique reflections above the 2 σ level and were 73% complete of a total of 18 909 possible reflections; the last shell (1.89–1.85-Å resolution) was 42% complete. The agreement of equivalent reflections within each film varied from 4.8% to 9.9% (R_{sym} values) whereas the agreement of measurement of equivalent reflections with their mean values from different films (R_{merge} values) varied from 8.6% to 11.1%. The crystal data are given in Table V.

Crystallographic Modeling and Refinement. The native enzyme coordinates¹³ were used for initial phasing of reflections for calculation of difference Fourier electron density at the active site region of the complex. The water molecules and the sulfate ion in the active site of the native structure were left out, and the other bound water molecules, calcium, and the sulfate ions in the native structure were retained for calculation of the difference map. Program TNT, a least-squares refinement program for macromolecular structures²⁸ was used for the calculation of maps and refinements. Five cycles of initial refinements consisting of four positional parameter refinements and one thermal parameter refinement were calculated on the unbiased model ($R = 25\%$) to account for the small differences in cell dimensions between native and inhibited enzymes before obtaining the initial difference Fourier map.

The Evans & Sutherland PS-330 graphics terminal and the program FRODO²⁹ were used for modeling of the inhibitor in the difference Fourier electron density in the active site. The modeling was done so as to be consistent both with the electron density from the unbiased Fourier maps and the known reaction chemistry

- (23) Nakajima, K.; Powers, J. C.; Ashe, B. M.; Zimmerman, M. Mapping the Extended Substrate Binding Site of Cathepsin G and Human Leukocyte Elastase. Studies with Peptide Substrates Related to the α_1 -Protease Inhibitor Reactive Site. *J. Biol. Chem.* 1979, 254, 4027–4032.
- (24) Bieth, J.; Spies, B.; Wermuth, C. G. Synthesis and Analytical Use of a Highly Sensitive and Convenient Substrate of Elastase. *Biochem. Med.* 1974, 11, 350–357.
- (25) Erlanger, B. F.; Kokowsky, N.; Cohen, W. Preparation and Properties of Two New Chromogenic Substrates of Trypsin. *Arch. Biochem. Biophys.* 1961, 95, 271–278.

- (26) Messerschmidt, A.; Pflugrath, J. W. Crystal Orientation and X-Ray Pattern Prediction Routines for Area-Detector Diffractometer Systems in Macromolecular Crystallography. *J. Appl. Crystallogr.* 1987, 20, 306–315.
- (27) Schwager, P.; Bartles, K.; Jones, A. Refinement of Setting Angles in Screenless Film Methods. *J. Appl. Crystallogr.* 1975, 8, 275–280.
- (28) Tronrud, D. E.; Ten Eyck, L. F.; Matthews, B. W. An Efficient General-Purpose Least-Squares Refinement Program for Macromolecular Structures. *Acta Crystallogr.* 1987, A43, 489–501.
- (29) Jones, T. A. A Graphics Model Building and Refinement System for Macromolecules. *J. Appl. Crystallogr.* 1978, 11, 268–272.

Table VI. Crystallographic Parameters and Final Refinement Statistics for the Structure of the Complex of PPE with 7-[(*N*-Tosylphenylalanyl)amino]-4-chloro-3-methoxyisocoumarin

crystal size, mm	0.5 × 0.4 × 0.5
cell dimensions, Å	a = 50.71, b = 58.13, c = 74.99
data collection temperature °C	-5
resolution range of data, Å	6.0–1.85
space group	<i>P</i> 2 ₁ 2 ₁ 2 ₁
effective resolution, ^a Å	1.96
no. of atoms/asymmetric unit	2152
no. of unique reflections above 2σ level	13872
% completeness of data	73
(<i>I</i> /σ <i>I</i>)	8.62
<i>R</i> factor ($R = \sum F_o - F_c / \sum F_o $)	0.169
overall temperature factor of 2116 atoms	17.22
in protein weighted as per electron count, Å ²	
overall temperature factor of the 36 inhibitor atoms, Å ²	30.21
σ of 1909 bond lengths, Å	0.012
σ of 2606 bond angles, deg	1.58
features of final residual difference density map, e/Å ³	
min height	-0.48
max height	0.40
σ	0.09
mean positional error, ^b Å	0.19

^aSwanson, S. M. Effective Resolution of Macromolecular X-Ray Diffraction Data. *Acta Crystallogr.* 1988, A44, 437–424. ^bLuzzati, V. Statistical Treatment of Errors in the Determination of Crystal Structures. *Acta Crystallogr.* 1952, 5, 802–810.

of isocoumarins. The densities clearly showed the covalent binding. Continuous density from Ser-195 O γ to the C1 atom of the isocoumarin ring, the densities for the methoxy group and the isocoumarin ring helped to model the inhibitor in the active site. There was moderate density for the chlorine atom and smeared densities for the tosyl group and the phenylalanyl side chain. This was probably due to the fact that PPE's active site is not as hydrophobic as that of HNE² and the inhibitor hydrophobic groups are thermally or statistically disordered in the PPE structure. The densities were good enough to model these hydrophobic groups.

Before starting further refinements of the complex with the inhibitor model in the active site, the positions of the Ca²⁺ and the SO₄²⁻ ions were checked in difference Fourier maps and were found to be conserved relative to the native structure. Most of the water molecules were also found to be close to their corresponding positions in the native structure.¹³ All were included with the native enzyme coordinates and the refinement was started with an initial temperature factor of 20 Å² for all nonhydrogen inhibitor atoms.

Refinements consisted of three cycles of atomic positional parameter refinements and a single cycle of atomic thermal (*B*) factor refinement alternately. Geometric constraints were introduced during positional parameter refinements. The *R* factor module (X-ray module) and geometry module were combined with a weighting for the *R* factor of 0.001, for bonds as 1.0, and for angles as 3.0. The TNT default values of weights for torsion, plane, and contact distance were employed. The geometric parameters for the ester bond between O γ of active site serine and the benzoyl carbonyl carbon atom of the inhibitor were taken from Schweizer

Table VII. Optimum and Refined Values for the Geometrical Parameters at the Covalent Bond Region between the Inhibitor and the Active Site Ser 195 Residue^a

geometric parameters	optimum	refined	geometric parameters	optimum	refined
C β -O γ	1.46	1.45	C1-O γ -C β	117.0	119.5
C1-O γ	1.35	1.33	C9-C1-O γ	116.0	121.8
C9-C1	1.40	1.42	C9-C1-O1	120.0	118.7
C1-O1	1.246	1.22	O1-C1-O γ	123.0	119.5

^aBond length in Å and angle in deg.

and Dunitz.³⁰ The Ser-195-inhibitor ester bond was treated analogously to a disulfide linkage. Geometric restraints used for the inhibitor complex at the covalent site are given in Table VI.

Additional water molecules were located in the difference Fourier maps at two stages during the course of the refinements and were identified by program TNTMAX (S. Swanson, unpublished results) and checked for proper geometry by the program WATER (R. Radhakrishnan, unpublished results). In total, 188 water molecules were introduced. After 109 cycles of refinement, the final *R* factor ($R = \sum ||F_o| - |F_c|| / \sum |F_o|$) was 0.169. The final standard deviations were 0.012 Å for 1909 bond lengths and 1.58° for 2606 bond angles in the sample. The refinement results are given in Table V. The refined parameters specific for the geometry at the covalent region of the enzyme inhibitor complex are given in Table VII. The overall temperature factor weighed as per electron count was 30.21 Å² for 36 inhibitor atoms and 17.22 Å² for 2109 atoms in the protein. The overall *B* values for Ser-195 and His-57 were 13.24 and 15.07 Å², respectively. The Phe and Tos groups have overall *B* values of 30.31 and 34.54 Å², respectively. These are indicative of only moderate hydrophobic interactions of these groups to the enzyme (Phe to Leu 151 and Tos to Tyr 35) although the hydrogen bonding interactions of the oxygens in the Tos group with enzyme and water molecules found in the active site add some stability to this group.

The RMS deviation between the native and the title structure for 802 backbone (NCCO) atoms is 0.23 (0.10) Å. When compared to the earlier determined 7-amino-4-chloro-3-methoxyisocoumarin complex with PPE, for 790 common backbone atoms the RMS deviation is 0.18 (0.07) Å and with the 4-chloro-3-ethoxy-7-guanidinoisocoumarin PPE complex, for 786 common backbone atoms, the RMS deviation is 0.17 (0.07) Å. With the 7-amino-3-(2-bromoethoxy)-4-chloroisocoumarin complex with PPE, the RMS deviation from the present structure is 0.16 (0.07) Å for 786 common backbone atoms.

Acknowledgment. This research was supported by a grant to Georgia Institute of Technology (HL20307) from the National Institutes of Health.

Registry No. 1, 62252-27-1; 2, 120218-97-5; 3, 120218-98-6; 4, 120218-99-7; 5, 120219-00-3; 6, 138695-66-6; 7, 138695-67-7; 8, 138695-68-8; 9, 138695-69-9; 10, 138695-70-2; 11, 138695-71-3; 12, 138695-72-4; 13, 138695-73-5; 14, 138695-74-6; 15, 138695-75-7; 16, 138695-76-8; 17, 138695-77-9; 18, 138695-78-0; 19, 99033-29-1; 20, 138695-79-1; 21, 126062-31-5; 22, 138695-80-4; 23, 138695-81-5; 24, 138695-82-6; 25, 126062-30-4; 26, 138695-83-7; elastase, 9004-06-2.

(30) Schweizer, W. B.; Dunitz, J. D. Structural Characteristics of the Carboxylic Ester Group. *Helv. Chim. Acta* 1982, 65, 1547–1554.